Supporting information: A metabolic perspective on competition and body size reductions with warming

Daniel C Reuman[1,2,*], **Robert D Holt**[3], **Gabriel Yvon-Durocher**[4,5]

1. *Division of Ecology and Evolution, Imperial College London, Silwood Park Campus, Ascot, SL5 7PY, U.K.*
2. *Laboratory of Populations, Rockefeller University, 1230 York Ave, New York, 10065, USA.*
3. *Department of Zoology, 223 Bartram Hall, PO Box 118525, University of Florida, Gainesville, FL 32611-8525, USA.*
4. *School of Biological and Chemical Sciences, Queen Mary University of London, London, E1 4NS, U.K.*
5. *Environment and Sustainability Institute, University of Exeter, Penryn, Cornwall, TR10 9EZ, U.K.*

*Correspondence author(s). d.reuman@imperial.ac.uk

1 Appendix: s and T dependence of parameters

We here provide details for the parameterizations described in the section "Phytoplankton: Parameterization" of the main text. Results for the dependence of μ_{max} and scaled assimilation affinity on cell size were from table 1 of Edwards *et al.* (2012), using their allometries common to freshwater and marine phytoplankton under N-limited growth. Confidence intervals provided by Edwards *et al.* (2012) were converted to standard errors by dividing half their length by 1.959964. The standard error of the scaling exponent of H_{gro} was computed as the square root of the sum of the squares of the standard errors of the scalings exponents of μ_{max} and scaled assimilation affinity, since the scaling exponent of H_{gro} was a difference of the two other exponents. This effectively assumes errors in the exponents are independent.

Results for $E_{\mu_{max}}$ from Bissinger *et al.* (2008) are from the first row of their table 1, converted from exponential dependencies to Arrhenius dependencies. Their confidence intervals were converted to the standard error for $E_{\mu_{max}}$ presented in the main text by converting an exponential dependence using each confidence interval endpoint to an Arrhenius dependence using the exponential prefactor 0.81 they provide (see their equation 2). The resulting confidence range for $E_{\mu_{max}}$ was converted to a standard error by dividing half its length by 1.959964.

Data on the viscosity of sea water at a range of temperatures were downloaded from the Chemical Hazards Response Information System of the U.S. Coastguard (`www.chrismanual.com/Intro/prop.htm`; downloaded data are reproduced in table S1). Temperatures were converted to °K and viscosities to $\mathrm{kg} \cdot \mathrm{m}^{-1} \cdot \mathrm{s}^{-1}$. A linear model was fitted with response variable $\log_e$ viscosity and predictor $\frac{1}{kT}$. The slope was 0.1781 (SE 0.001) and the intercept was -13.8738 (standard error 0.0405). The linear model explained 99.98% of the variation in $\log_e$ viscosity.

2 Appendix: a specific T dependence of H_{gro}

Equation 9 of the main text establishes a power law dependence of H_{gro} on cell size, s. Although not needed for the results of the main text, we here provide theoretical and empirical arguments supporting a particular T dependence of H_{gro}. By the equation for H_{gro} in equations 6 in the main text, it suffices to understand the T dependencies of H_{up}, Q_{min}, and V_{max}; the T dependence of μ_{max} is in the main text.

We begin with theoretical arguments for H_{up} and V_{max}, largely taken from Aksnes & Egge (1991). Nutrients are actively transported into a cell by ion uptake sites on the cell surface. Aksnes & Egge (1991) mechanistically modeled this process using the same reasoning behind the Holling type II functional response used in predator-prey models (Holling, 1959). They obtained a formula for uptake rate, as limited by encounters between ions and uptake sites, and by the time it takes for an uptake site to process an ion once encountered. Converting their formulas to our notation provides

$$V_{max} = \frac{n}{h} \tag{1}$$

and

$$H_{up} = \frac{1}{hAv}, \tag{2}$$

where n is the number of uptake sites occurring on the cell surface (sites $\cdot$ cell^{-1}), h is the time required for an uptake channel to process an ion, i.e., the "handling time" (days), A is the capture area of an uptake site (μm^2), and v is a "mass transfer coefficient" which is an average equivalent relative velocity between ions and uptake sites (μm $\cdot$ day^{-1}). We can model the s and T dependence of V_{max} and H_{up} by modeling the s and T dependence of n, h, A and v. This is the strategy used by Litchman *et al.* (2007) and Verdy *et al.* (2009), though they did not include temperature dependence.

We assume A is independent of both s and T. We assume n is proportional to cell surface area and independent of T, so

$$n \propto s^{2/3}. \tag{3}$$

The handling time, h is the time required for the biochemical reactions of ion uptake, and as such seems likely to have inverse Arrhenius temperature dependence. We assume h does not depend systematically on s, so

$$h \propto \exp\left(\frac{E_h}{kT}\right), \tag{4}$$

with $E_h > 0$. Aksnes & Egge (1991) used the approximation

$$v = \frac{D}{r}, \tag{5}$$

where D is the coefficient of molecular diffusion for the nutrient (μm^2 $\cdot$ day^{-1}), r is the equivalent spherical radius of the cell (μm), and we assume nutrient transport to the cell is largely via diffusion as opposed to cell motion through the medium. The Einstein-Stokes equation gives

$$D \propto \frac{T}{\eta}, \tag{6}$$

where η is the dynamic viscosity of the medium. Aksnes & Egge (1991) realized that temperature influenced D as described in this proportionality, and then in turn influenced v and H_{up} as described in equations 5 and 2, however, they said "as the temperature-dependent viscosity also influences diffusion, the overall influence of temperature on molecular diffusion is not straightforward." But the influence of T on viscosity is known:

$$\eta \propto \exp\left(\frac{E_\eta}{kT}\right), \tag{7}$$

where $E_\eta = 0.1781$ (Appendix S1). Combining equations 5, 6 and 7, we have

$$v \propto s^{-1/3} T \exp\left(\frac{-E_\eta}{kT}\right), \tag{8}$$

so that dependencies on s and T of n, h, A and v have been modeled.

Substituting the expressions for n, h, and v (equations 3, 4, and 8) into equations 1 and 2, we have

$$V_{max} \propto s^{2/3} \exp\left(\frac{-E_h}{kT}\right) \propto s^{2/3} \exp\left(\frac{E_h(T-T_0)}{kTT_0}\right) \tag{9}$$

and

$$H_{up} \propto \frac{s^{1/3} \exp\left(\frac{-E_{H_{up}}}{kT}\right)}{T} \propto \frac{s^{1/3} \exp\left(\frac{E_{H_{up}}(T-T_0)}{kTT_0}\right)}{T} \tag{10}$$

where

$$E_{H_{up}} = E_h - E_\eta. \tag{11}$$

The cell-size scaling exponents predicted here (2/3 for V_{max} and 1/3 for H_{up}) are similar to the values obtained empirically by Edwards *et al.* (2012) (see their table 1, "common slope" column); they got scaling exponent for V_{max} for N uptake equal to 0.82 (SE 0.077) and scaling exponent for H_{up} for N uptake equal to 0.33 (SE 0.041). See also Litchman *et al.* (2007), who obtained similar scaling exponents. The agreement of theory with empirical results on cell-size scaling exponents lends credence to theoretical predictions for temperature dependence.

We tested the theoretically predicted functional form for the temperature dependence of H_{up} and obtained an estimate for $E_{H_{up}}$ via a metastudy. We found in the literature 79 measurements of H_{up} for 16 different species or groups at temperatures ranging from 1°C to 29°C; all data and references are in table S3. Cell-size measurements generally were not available. We fitted a linear mixed-effects model (Pinheiro & Bates, 2000), $y_{kl} = E_{H_{up}} x_{kl} + b + \delta_k + \epsilon_{kl}$, where k indexes unique species-study combinations in the data, l indexes measurements (at different temperatures) taken within a species-study combination, y_{kl} represents $\log_e(H_{up}) + log_e(T)$ for the kl-th data point, and x_{kl} represents $(T_{kl} - T_0)/(kT_{kl}T_0)$ where T_{kl} is the temperature (°K) for the kl-th data point and $T_0 = 293.15$°K. The random factor δ_k, which takes an independent value for each species-study combination, is normally distributed with a variance parameter determined in fitting. The δ_k account for differences among species and methodological differences among studies. The ϵ_{kl} term is a normally distributed residual error term. The main result of this fitting was an estimate $E_{H_{up}} = 0.277$ (SE 0.084), but we also obtained estimates for the δ_k and plotted $y_{kl} - \delta_k$ against $E_{H_{up}} x_{kl} + b$, using the estimated values of the parameters $E_{H_{up}}$ and b, to demonstrate that linearity of the fixed effect was supported (figure S1A). The package lme4 in the R programming language was used to fit the model. The activation energy for V_{max} can be obtained from equation 11, i.e., $E_{V_{max}} = E_h = E_{H_{up}} + E_\eta = 0.456$. The standard error on this estimate is practically the same as that for $E_{H_{up}}$ because the standard error for E_η is very small (Appendix S1).

To assess the T dependence of Q_{min}, we carried out another metastudy. We found in the literature 41 measurements of Q_{min} for 7 different species or groups at temperatures ranging from 3°C to 25°C; all data and references are in table S4. Cell-size measurements generally were not available. We fitted a linear mixed-effects model (Pinheiro & Bates, 2000), $y_{kl} = E_{Q_{min}} x_{kl} + b + \delta_k + \epsilon_{kl}$, where k indexes unique species-study combinations in the data, l indexes measurements (at different temperatures) taken within a species-study combination, y_{kl} represents $\log_e(Q_{min})$ for the kl-th data point, and x_{kl} represents $(T_{kl} - T_0)/(kT_{kl}T_0)$. The random factor δ_k and the residual error ϵ_{kl} are conceptually the same as in the mixed-effects model for H_{up} described above. The main result of this fitting was an estimate

$E_{Q_{min}} = -0.230$ (SE 0.056), but we also obtained estimates for the δ_k and plotted $y_{kl} - \delta_k$ against $E_{Q_{min}} x_{kl} + b$, using the estimated values of the parameters $E_{Q_{min}}$ and b, to demonstrate that linearity of the fixed effect was supported (figure S1B). Thus Q_{min} has the form

$$Q_{min} \propto s^{e_{Q_{min}}} \exp\left(\frac{E_{Q_{min}}(T - T_0)}{kTT_0}\right), \tag{12}$$

with $E_{Q_{min}} = -0.230$, where the power-law cell-size dependence used here is supported by the results of Edwards *et al.* (2012), with their value $e_{Q_{min}} = 0.84$ (SE 0.046).

Combining the dependencies for H_{up}, Q_{min}, V_{max}, and μ_{max} gives

$$H_{gro} \propto \frac{s^{e_{H_{up}} + e_{Q_{min}} + e_{\mu_{max}} - e_{V_{max}}} \exp\left(\frac{(E_{H_{up}} + E_{Q_{min}} + E_{\mu_{max}} - E_{V_{max}})(T - T_0)}{kTT_0}\right)}{T}, \tag{13}$$

where the value $e_{H_{gro}} = e_{H_{up}} + e_{Q_{min}} + e_{\mu_{max}} - e_{V_{max}} = \frac{1}{3} + 0.84 - 0.28 - \frac{2}{3} = 0.227$ is close to the value derived from the regressions of Edwards *et al.* (2012) (table 1 of the main text).

3 Appendix: derivative of G with respect to T

The invasion fitness, G, of an invader of cell size s_{in} into a resident of cell size s_{re} was derived in the main text (main text equation 11). The derivative of G with respect to T was needed to establish the effects of temperature on the relative competitive abilities of differently sized plankton cells. The derivative is computed here:

$$\frac{\partial G}{\partial T} = \frac{\frac{\partial \mu_{max}}{\partial T}(s_{in}, T) g_m(s_{re}) s_{re}^{e_{H_{gro}}}}{D} \tag{14}$$

$$- \frac{\mu_{max}(s_{in}, T) g_m(s_{re}) s_{re}^{e_{H_{gro}}} s_{in}^{e_{H_{gro}}} \frac{\partial \mu_{max}}{\partial T}(s_{re}, T)}{D^2} \tag{15}$$

where

$$D = g_m(s_{re}) s_{re}^{e_{H_{gro}}} + s_{in}^{e_{H_{gro}}} (\mu_{max}(s_{re}, T) - g_m(s_{re})). \tag{16}$$

Substituting $\frac{\partial \mu_{max}}{\partial T} = \frac{E_{\mu_{max}}}{kT^2} \mu_{max}$ and simplifying gives;

$$\frac{\partial G}{\partial T} = \frac{\mu_{max}(s_{in}, T) \frac{E_{\mu_{max}}}{kT^2} g_m(s_{re})^2 s_{re}^{e_{H_{gro}}} (s_{re}^{e_{H_{gro}}} - s_{in}^{e_{H_{gro}}})}{D^2}. \tag{17}$$

The denominator, D^2, is strictly positive because $m = g_m$ is positive and $\mu_{max}(s_{re}) - g_m(s_{re}) > 0$ is a condition for the resident to have become established in the first place. Therefore the sign of $\frac{\partial G}{\partial T}$ is the same as the sign of the numerator of equation 17, which is positive for $s_{re} > s_{in}$ and negative for $s_{re} < s_{in}$ since $e_{H_{gro}} > 0$.

4 Appendix: R^* for the case $m = k_m s^{e_m}$

In section "Phytoplankton: Model analysis and results" of the main text, the case in which mortality is $m = g_m(s) = k_m s^{e_m}$ is considered, and it is stated that an evolutionarily stable size (ESS) exists under certain conditions. We here demonstrate this and compute the ESS. Equation 12 of the main text is minimized with changes in s exactly when

$$\tilde{R}^* = \frac{s^{e_{H_{gro}}+e_m}}{f_{\mu_{max}}(T)s^{e_{\mu_{max}}} - k_m s^{e_m}} \tag{18}$$

is minimized, where we use the shorthand $f_{\mu_{max}} = k_{\mu_{max}} \exp\left(\frac{E_{\mu_{max}}(T-T_0)}{kTT_0}\right)$. Taking derivatives and simplifying gives

$$\frac{\partial \tilde{R}^*}{\partial s} = \frac{s^{e_{H_{gro}}+e_m-1}((e_m + e_{H_{gro}} - e_{\mu_{max}})f_{\mu_{max}}(T)s^{e_{\mu_{max}}} - e_{H_{gro}}k_m s^{e_m})}{(f_{\mu_{max}}(T)s^{e_{\mu_{max}}} - k_m s^{e_m})^2}. \tag{19}$$

Cell size s is viable only if the denominator of this expression is greater than zero. The sign of equation 19 is the same as the sign of its numerator, which in turn is the same as the sign of

$$(e_m + e_{H_{gro}} - e_{\mu_{max}})\frac{f_{\mu_{max}}(T)s^{e_{\mu_{max}}}}{k_m s^{e_m}} - e_{H_{gro}}, \tag{20}$$

since $k_m s^{e_m} > 0$ and $s^{e_{H_{gro}}+e_m-1} > 0$.

If $e_{\mu_{max}} < e_m$ then equation 20 is always positive, because then $e_m + e_{H_{gro}} - e_{\mu_{max}} > e_{H_{gro}}$, and we already know the quotient in equation 20 is greater than 1 for viable cell sizes, s. So in that case, $\partial R^*/\partial s > 0$ for all viable s and we have runaway selection to small sizes. There is also a maximum viable size

$$s_{max} = \left(\frac{f_{\mu_{max}}(T)}{k_m}\right)^{\frac{1}{e_m - e_{\mu_{max}}}} \tag{21}$$

if $e_{\mu_{max}} < e_m$.

If $e_m < e_{\mu_{max}} - e_{H_{gro}}$, then $e_m + e_{H_{gro}} - e_{\mu_{max}} < 0$, and equation 20 is always negative because $e_{H_{gro}} > 0$. So in that case, $\partial R^*/\partial s < 0$ for all viable s, and we have runaway selection to large sizes. There is a minimum viable size

$$s_{min} = \left(\frac{k_m}{f_{\mu_{max}}(T)}\right)^{\frac{1}{e_{\mu_{max}} - e_m}} \tag{22}$$

if $e_m < e_{\mu_{max}}$.

If $e_{\mu_{max}} - e_{H_{gro}} < e_m < e_{\mu_{max}}$, then equation 20 has a root,

$$s_{ESS} = \left(\frac{e_{H_{gro}}k_m}{(e_m + e_{H_{gro}} - e_{\mu_{max}})f_{\mu_{max}}(T)}\right)^{\frac{1}{e_{\mu_{max}} - e_m}}. \tag{23}$$

Because equation 20 is a monotonically increasing function of s for $e_{\mu_{max}} - e_{H_{gro}} < e_m < e_{\mu_{max}}$, it is negative for $s < s_{ESS}$ and positive for $s > s_{ESS}$, so s_{ESS} is a local and global minimum

of $\tilde{R}^*$ and therefore of R^*.

5 Appendix: The equilibrium assumption

The use of R^* and G made in the main text in analyzing the phytoplankton model depends on the assumption that equilibria are stable. This seems likely because model nutrients are supplied at a constant rate. Nevertheless, we tested the assumption numerically using a Monte Carlo method, for a wide range of parameters encompassing biologically reasonable values. Edwards *et al.* (2012) provide allometries of the form $y = ks^e$ for $y = Q_{min}$, μ_{max}, H_{up}, and V_{max}, giving estimates and confidence intervals for $\log_{10}(k)$ and e in all cases. Confidence intervals were converted to standard errors by dividing half their length by 1.959964. Montagnes & Franklin (2001) provide an allometry for Q_{max}, with estimates and standard errors for $\log_{10}(k)$ and e. See table S2 for all values taken from these references. On each Monte Carlo run, the parameters $\log_{10}(k)$ and e for each allometry were drawn from normal distributions with mean equal to the estimated value from Edwards *et al.* (2012) or Montagnes & Franklin (2001) and standard deviation equal to twice the standard error reported in those references. Twice the standard error was used to add a buffer of additional uncertainty. Cell sizes $\log_{10}(s)$ were drawn randomly and uniformly between 0 and 8 and the allometries resulting from the randomly generated values of the k and e for each allometry were used to generate values for Q_{min}, μ_{max}, H_{up}, V_{max}, and Q_{max}. When Q_{max} was less than Q_{min} the values were swapped. Input nutrient concentration $R_0 = 40$ was used following Litchman *et al.* (2009). Nutrient supply rates, d, were taken as a uniformly distributed random variable between 0.05 and 0.95 divided by a uniformly distributed random variable between 1 and 50. The first variable represents replacement fractions in mixing events and the second represents mixing-event periods; both ranges are from Litchman *et al.* (2009). Mortality, m, was a uniform random variable between 1×10^{-4} and 0.02. The parameter μ_∞ was established by solving the μ_{max} equation in equations 6 in the main text for μ_∞. For each of 10,000 runs, equilibria were computed following the equations of Verdy *et al.* (2009). When equilibria existed (9,464 runs), the system Jacobian was computed at the equilibrium. In all cases, the real parts of the eigenvalues of the Jacobian were negative, indicating stability. Temperature was not accounted for in this analysis because data are not available on the temperature dependence of all model parameters; nevertheless it seems unlikely model equilibria are ever unstable for biologically reasonable parameters given the wide uncertainties incorporated above and the result that every simulated equilibrium was stable. We find it plausible to expect that local stability is a mathematical necessity for any equilibrium, but we do not know of a proof of this.

6 Appendix: Non-equilibrium dynamics

The R^* and invasion-fitness approach as described here is valid only when the equilibrium is stable, but in contrast to the phytoplankton model (Appendix S5), an equilibrium of the Rosenzweig-MacArthur model need not be stable. A Hopf bifurcation occurs at a parameter boundary given by Vasseur & McCann (2005); past the boundary, the model has a stable limit cycle. Invasion fitness into a resident exhibiting limit-cycle oscillations can still be

computed by averaging the growth rate of the putative invader over the limit-cycle resource density driven by the resident (see, e.g., Klausmeier, 2008; Kooi & Troost, 2006; Litchman *et al.*, 2009). A non-equilibrium approach will require all model parameters to be written as functions of s and T instead of just those appearing in expressions for R^* and G, but this should be possible for the Rosenzweig-MacArthur model if α and t_h can be described. Savage *et al.* (2004) published theory and data on body mass and temperature dependence of r and K, and Vasseur & McCann (2005) cover the body mass and temperature dependence of r as well as m and μ_{max}. An important direction for future work will be elucidating the thermal dimension of non-equilibrial competitive interactions.

References

Aksnes, D. & Egge, J. (1991) A theoretical model for nutrient uptake in phytoplankton. *Marine Ecology Progress Series*, **70**, 65–72.

Bissinger, J., Montagnes, D., Sharples, J. & Atkinson, D. (2008) Predicting marine phytoplankton maximum growth rates from temperature: Improving the Eppley curve using quantile regression. *Limnology and Oceanography*, **53**, 487–493.

Edwards, K., Thomas, M., Klausmeier, C. & Litchman, E. (2012) Allometric scaling and taxonomic variation in nutrient utilization traits and maximum growth rate of phytoplankton. *Limnology and Oceanography*, **57**, 554–566.

Holling, C. (1959) The components of predation as revealed by a study of small-mammal predation of the European pine sawfly. *Canadian Entomologist*, **91**, 293–320.

Klausmeier, C. (2008) Floquet theory: a useful tool for understanding nonequilibrium dynamics. *Theoretical Ecology*, **1**, 153–163.

Kooi, B. & Troost, T. (2006) Advantage of storage in a fluctuating environment. *Theoretical Population Biology*, **70**, 527–541.

Litchman, E., Kalusmeier, C., Schofield, O. & Falkowski, P. (2007) The role of functional traits and trade-offs in structuring phytoplankton communities: scaling from cellular to ecosystem level. *Ecology Letters*, **10**, 1170–1181.

Litchman, E., Kalusmeier, C. & Yoshiyama, K. (2009) Contrasting size evolution in marine and freshwater diatoms. *Proceedings of the National Academy of Sciences*, **106**, 2665–2670.

Montagnes, D. & Franklin, D. (2001) Effect of temperature on diatom volume, growth rate, and carbon and nitrogen content: reconsidering some paradigms. *Limnology and Oceanography*, **46**, 2008–2018.

Pinheiro, J. & Bates, D. (2000) *Mixed-Effects Models in S and S-Plus*. Springer, New York.

Savage, V., J.M., G., Brown, J., West, G. & Charnov, E. (2004) Effects of body size and temperature on population growth. *The American Naturalist*, **163**, 429–441.

Vasseur, D. & McCann, K. (2005) A mechanistic approach for modelling temperature-dependent consumer-resource dynamics. *American Naturalist*, **166**, 184–198.

234 Verdy, A., Follows, M. & Flierl, G. (2009) Optimal phytoplankton cell size in an allometric model.
235 *Marine Ecology Progress Series*, **379**, 1–12.

Tables

Table 1 Viscosity of sea water at a range of temperatures. Data were taken from the Chemical Hazards Response Information System of the U.S. Coast Guard (www.chrismanual.com/Intro/prop.htm), and are for "standard" sea water containing 35g salts per kg of solution.

Temp. (°F)	Visc. (Centipoise)	Temp. (°K)	Visc. ($kg \cdot m^{-1} \cdot s^{-1}$)
30	1.88	272.04	0.00188
40	1.61	277.59	0.00161
50	1.40	283.15	0.00140
60	1.21	288.71	0.00121
70	1.06	294.26	0.00106
80	0.92	299.82	0.00092
90	0.82	305.37	0.00082
100	0.73	310.93	0.00073

Table 2 Parameter estimates used in Monte Carlo simulations (see Appendix S5). Values from Edwards *et al.* (2012) are from their table 1, using values fitted to pooled freshwater and marine data. Values from Montagnes & Franklin (2001) are from their table 3.

Parameter	Estimate	SE	Source
$e_{Q_{min}}$	0.84	0.046	Edwards *et al.* (2012)
$\log_{10}(k_{Q_{min}})$	-9.0	0.128	Edwards *et al.* (2012)
$e_{\mu_{max}}$	-0.28	0.018	Edwards *et al.* (2012)
$\log_{10}(k_{\mu_{max}})$	0.65	0.059	Edwards *et al.* (2012)
$e_{H_{up}}$	0.33	0.041	Edwards *et al.* (2012)
$\log_{10}(k_{H_{up}})$	-0.61	0.138	Edwards *et al.* (2012)
$e_{V_{max}}$	0.82	0.077	Edwards *et al.* (2012)
$\log_{10}(k_{V_{max}})$	-8.0	0.281	Edwards *et al.* (2012)
$e_{Q_{max}}$	0.809	0.011	Montagnes & Franklin (2001)
$\log_{10}(k_{Q_{max}})$	-8.03	0.039	Montagnes & Franklin (2001)

Figures

A, B

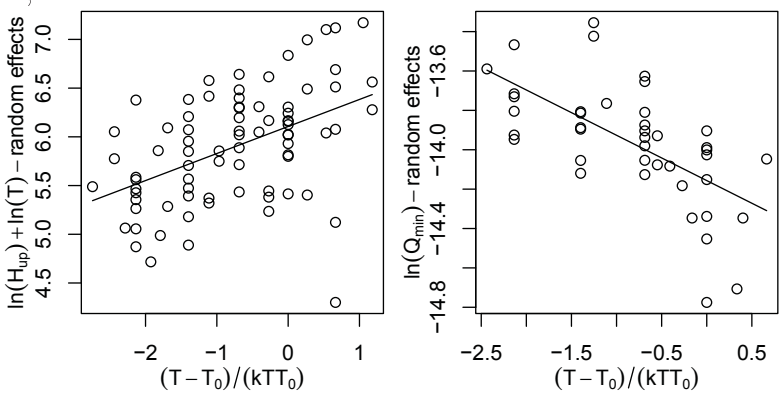

Fig. 1 Plots of metastudy data, corrected for random effects; lines have fixed-effect slopes and intercepts (see Appendix S2).

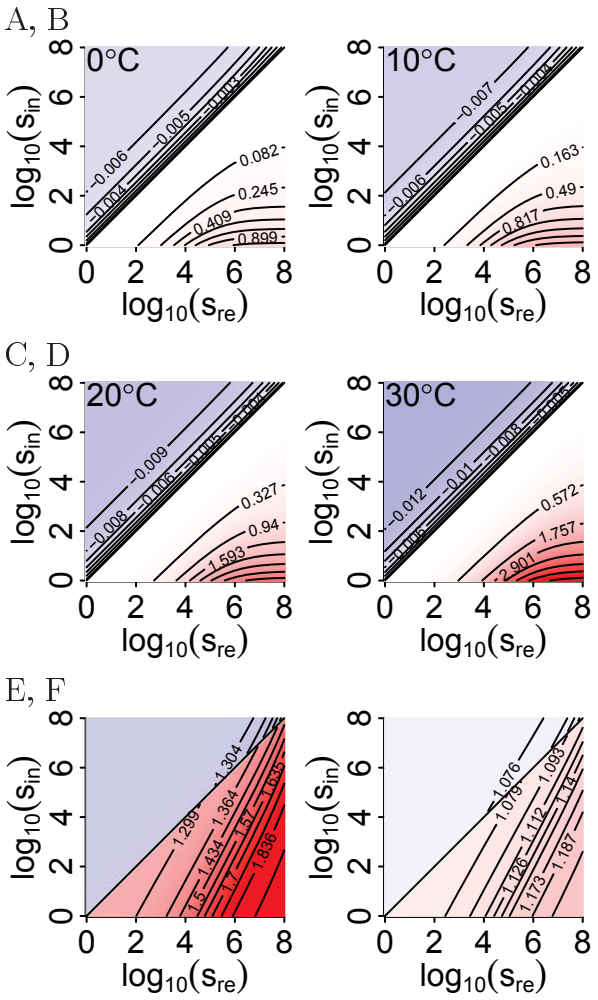

Fig. 2 (A-D) Pairwise invasibility plots at different temperatures for $m = 0.01 \exp(E_m(T - T_0)/(kTT_0))$ with $E_m = 0.1781$. These plots are analogous to figure 4A-D of the main text, but for a different model of m. (E-F) Ratios of pairwise invasibilities at different temperatures for the same m. These plots are analogous to figure 4E-F of the main text. Plots show $G(s_{in}, s_{re}, T_1)/G(s_{in}, s_{re}, T_2)$ for $T_1 = 20°\text{C}$ and $T_2 = 10°\text{C}$ (E) and for $T_1 = 23°\text{C}$ and $T_2 = 20°\text{C}$ (F). The same result of accentuated invasion fitness of smaller invaders at warmer temperatures was also true for $k_m = 0.0001, 0.001$, and 0.02.